JPET Fast Forward. Published on August 21, 2012 as DOI: 10.1124/jpet.112.197954

Title Page

Establishing the relationship between *in vitro* potency, pharmacokinetic and pharmacodynamic parameters in a series of orally available, hydroxyethylamine-derived β-secretase inhibitors

Stephen Wood, Paul H. Wen, Jianhua Zhang, Li Zhu, Yi Luo, Safura Babu-Khan[1], Kui Chen, Roger Pham, Joel Esmay, Thomas A. Dineen, Matthew R. Kaller, Matthew M. Weiss, Stephen A. Hitchcock[2], Martin Citron[3], Wenge Zhong, Dean Hickman, and Toni Williamson[4]

Department of Neuroscience (S.W., P.H.W., J.Z., L.Z., Y.L., S.B., M.C. and T.W.), Department of Medicinal Chemistry, (M.R.K., S.A.H. and W.Z.), Department of Molecular Structure and Characterization (K.C.), Department of Pharmacokinetics and Drug Metabolism (R.P., J.E. and D.H.), Amgen, Inc., Thousand Oaks, CA and Department of Medicinal Chemistry, (T.A.D. and M.M.W.), Amgen, Inc., Cambridge, MA

JPET Fast Forward. Published on August 21, 2012 as DOI: 10.1124/jpet.112.197954
This article has not been copyedited and formatted. The final version may differ from this version.

Running Title Page

PK/PD evaluation of HEA-derived β-secretase inhibitors

Corresponding author: Stephen Wood, One Amgen Center Drive, 29-2-B, Thousand Oaks, CA 91320; Tel: 805-447-7065. Fax: 805-480-1358. E-mail: stephenw@amgen.com

Number of text pages: 33

Number of tables: 1

Number of figures: 6

Number of references: 33

Number of words in Abstract: 242

Number of words in Introduction: 526

Number of words in Discussion: 1103

Non-standard abbreviations: AD, Alzheimer's Disease; Aβ, amyloid-β peptide; HEA, hydroxythethylamine; APP, amyloid precursor protein; BACE1, β-site APP-cleaving enzyme 1; P-gp, P-glycoprotein; Compound 1, N-((2S,3R)-1-(benzo[d][1,3]dioxol-5-yl)-3-hydroxy-4-(((S)-6'-neopentyl-3',4'-dihydrospiro[cyclobutane-1,2'-pyrano[2,3-b]pyridin]-4'-yl)amino)butan-2-yl)-2-methoxyacetamide; Compound 2, (R)-N-((2S,3R)-3-hydroxy-4-(((S)-6'-neopentyl-3',4'-dihydrospiro[cyclobutane-1,2'-pyrano[2,3-b]pyridin]-4'-yl)amino)-1-(3-(thiazol-2-yl)phenyl)butan-2-yl)-2-methoxypropanamide

Recommended section assignment: Neuropharmacology

JPET Fast Forward. Published on August 21, 2012 as DOI: 10.1124/jpet.112.197954
This article has not been copyedited and formatted. The final version may differ from this version.

Abstract

Sequential proteolytic cleavage of the amyloid precursor protein (APP) by beta-site APP-cleaving enzyme 1 (BACE1) and the gamma-secretase complex produces the peptide Aβ which is believed to play a critical role in the pathology of Alzheimer's disease (AD). The aspartyl protease BACE1 catalyzes the rate-limiting step in the production of Aβ, and as such it is considered to be an important target for drug development in AD. The development of a BACE1 inhibitor therapeutic has proven difficult. The active site of BACE1 is relatively large. Consequently, to achieve sufficient potency, many BACE1 inhibitors have required unfavorable physicochemical properties such as high molecular weight and polar surface area that are detrimental to efficient passage across the blood-brain barrier. Using a rational drug design approach we have designed and developed a new series of hydroxyethylamine (HEA)-based inhibitors of BACE1 capable of lowering Aβ levels in brains of rats after oral administration. Herein we describe the *in vitro* and *in vivo* characterization of 2 of these molecules as well as the overall relationship of compound properties (e.g. *in vitro* permeability, P-glycoprotein (P-gp) efflux, metabolic stability and pharmacological potency) to the *in vivo* pharmacodynamic effect with more than 100 compounds across the chemical series. We demonstrate that high *in vitro* potency for BACE1 was not sufficient to provide central efficacy. A combination of potency, high permeability, low P-gp mediated efflux and low clearance was required for compounds to produce robust central Aβ reduction after oral dosing.

Introduction

Alzheimer's disease (AD), a progressive neurodegenerative disorder, is the most common form of dementia that affects 4-8% of the elderly population worldwide. The neuropathological features of AD are the presence of extracellular amyloid plaques and intracellular neurofibrillary tangles (NFT) in the hippocampus and cortical grey matter of the brain (Citron, 2010). The core constituent of the amyloid plaques, also known as senile plaques, is a small 4 kDa amyloid-β peptide (Aβ). Assembly and aggregation of Aβ into soluble oligomers and amyloid fibrils is believed by many to play a key role in the etiology of AD and therefore strategies to lower Aβ production have been pursued with great interest in the AD field over the past 2 decades (Hardy and Selkoe, 2002). Aβ is a fragment of a much larger precursor protein, the amyloid precursor protein (APP). Sequential proteolytic cleavage of APP by beta-site APP-cleaving enzyme 1 (BACE1) and the gamma-secretase complex produces the Aβ peptide. The aspartyl protease BACE1 catalyzes the rate-limiting step in the production of Aβ, and is therefore considered to be an important target for drug development in AD (Vassar and Kandalepas, 2011).

The development of BACE1 inhibitor therapeutics has been challenging. The x-ray structure of BACE1 co-crystallized with a transition-state analog inhibitor has been useful for the design of BACE1 inhibitors with good *in vitro* potency (Hong et al., 2000). However, the large active site of the enzyme has made it difficult to find small molecules that are both potent inhibitors of the enzyme and also possess the appropriate pharmacokinetic properties to enable inhibition of Aβ production in the brain (Hong et

al., 2000; Stachel et al., 2009; Turner et al., 2001). Nonetheless, over the last decade, much progress has been made across industry and academia in designing BACE1 inhibitors with physicochemical properties that allow for effective Aβ lowering *in vivo* (Ghosh et al., 2012). In the last few years, a number of groups have succeeded in making potent BACE1 inhibitors capable of lowering central Aβ in APP transgenic mice, rats, guinea pigs, monkeys and man (Chakrabarti et al., 2010; Charrier et al., 2009; Fukumoto et al., 2010; Malamas et al., 2010; May et al., 2011; Sankaranarayanan et al., 2009; Truong et al., 2010). Using a rational drug design approach we have designed and developed a new series of hydroxyethylamine-based inhibitors of BACE1 that can potently reduce Aβ levels in brain and cerebrospinal fluid (CSF) after oral administration (Dineen et al., 2012; Kaller et al., 2012; Weiss et al., 2012).

In this report, we describe the *in vitro* and *in vivo* characterization of 2 of these molecules as well as the overall relationship of compound properties (e.g. *in vitro* permeability, P-gp mediated efflux, metabolic stability and pharmacological potency) to the *in vivo* pharmacodynamic effect across the chemical series. We demonstrate that high *in vitro* potency for BACE1 was not sufficient to provide central efficacy. In fact, no single parameter on its own was able to provide an absolute *in vitro* surrogate for *in vivo* potency; compounds required a balanced PK profile that consisted of low metabolic clearance, high permeability and low efflux in order to produce robust central Aβ reduction after oral dosing.

Materials and Methods

Human recombinant BACE1 enzymatic assay in FRET format

The extracellular domain of human BACE1 was expressed in CHO cells as previously described (Vassar et al., 1999). The enzymatic activity of recombinant BACE1 was measured using a fluorescence resonance energy transfer (FRET) assay according to published methods (Yang et al., 2004). The substrate was a synthetic peptide that contained the BACE1 cleavage site (Turner et al., 2001) and fluorophore and quencher dyes at the termini of the peptide. Compounds were pre-incubated with the enzyme at pH 4.5 for 60 min at room temperature, and the subsequent reaction was initiated by addition of the substrate. After one hour, the reaction was stopped by raising the pH above the enzyme active range (> 7). The enhancement of fluorescence intensity upon enzymatic cleavage of the FRET substrate was measured on a Safire II microplate reader (Tecan, Männedorf, Switzerland).

Passive permeability and rat P-gp mediated efflux ratio

Transcellular transport was measured using LLC-PK1 cell monolayers as described previously (Booth-Genthe et al., 2006) with slight modifications. LLC-PK1 cells were plated on porous (1.0 µm) polycarbonate 96-well membrane filters (Millipore Corp., Billerica, MA) in a feeder tray of medium. The transport experiment was initiated on the 6th day after plating by replacing the buffer in each compartment with Hepes-buffered Hank's balanced salt solution containing 0.1% BSA with and without 5 µM compound in triplicate. Transcellular transport of ^{3}H-Digoxin at 0.5 µM was also evaluated as a positive control for P-gp. The monolayer integrity was also tested using

JPET Fast Forward. Published on August 21, 2012 as DOI: 10.1124/jpet.112.197954
This article has not been copyedited and formatted. The final version may differ from this version.

^{14}C-Mannitol, a paracellular diffusion indicator. After 2 hours, aliquots were taken from both apical and basolateral chambers and analyzed for drug by LC-MS/MS on an API4000 (Applied Biosystem, Foster City, CA) triple quadruple mass spectrometer interfaced with turbo IonSpray operated in positive mode using Analyst 1.4.2 software.

Efflux was measured in LLC-PK1 cells transfected with rat mdr1A/1B. Efflux ratio (ER) was calculated from the basolateral-to-apical permeability divided by the apical-to-basolateral permeability.

Microsomal stability – Intrinsic clearance in rat liver microsomes (RLM CL_{int})

Compounds (1 µM) were incubated with rat liver microsomes (0.25 mg/ml in 67 mM phosphate buffer, pH 7.4) from rat at 37°C for 30 minutes with or without 1 mM NADPH in a total volume of 0.2 ml. The final concentration of DMSO in the incubation was < 0.1%. Incubations were stopped by addition of 200 µl of ice-cold acetonitrile containing 0.5% formic acid and an internal standard (500 ng/ml) followed by centrifugation at 3,100 rpm for 20 minutes. The supernatants were analyzed directly (without any further sample clean-up) by high performance liquid chromatography (HPLC) and mass spectrometric detection.

Plasma protein binding

Compounds were spiked into plasma to a final concentration of 5 µg/ml (0.1% DMSO final), gently mixed and incubated at 37°C for 15 minutes. Aliquots of incubated plasma (0.5 ml) were transferred to polycarbonate tubes and centrifuged at 627,000 RCF for 3 h at 37°C. The centrifugation process pellets 99.2% of plasma proteins

(Nakai, 2004). The supernatants (0.1 ml) were transferred into 0.1 ml of blank 4% plasma in plasma water. An additional aliquot of each compound spiked plasma sample was diluted 1:50 in plasma water (Bioreclamation Inc.) and retained for analysis. Standard curve and analytical quality control (QC) samples were constructed in 2% plasma in plasma water. 50 µl of internal standard (500 ng/ml in acetonitrile) was added to 50 µl of unknown samples, standards and QCs. An additional 250 µl acetonitrile ensured precipitation of protein with vortexing. Samples, standards and QCs were centrifuged to pellet proteins and a 250 µl aliquot removed to a clean deep well plate. Samples were either analyzed directly or following drying under nitrogen and reconstitution in 0.1 ml methanol/water (1:1 v:v).

Whole-cell Aβ assay

HEK293 (human embryonic kidney cells) stably transfected with APP695 containing the Swedish familial Alzheimer's disease (FAD) mutation ($APP_{K595N/M596L}$) were used to test compounds in a whole-cell assay. Cells were incubated 16-18 h with compounds at concentrations ranging from 0.0005 to 10 µM. Conditioned media was removed and analyzed for Aβ levels as described below.

Aβ40 measurements and data analysis

Samples were analyzed for Aβ40 levels by sandwich immunoassay according to a previously published protocol (Best et al., 2005). Briefly, 96-well avidin plates (MesoScale Discovery, Inc. (MSD)) were coated with biotinylated-anti-Aβ antibody, 4G8 (Covance) which recognizes an epitope within the mid-region of the Aβ peptide (amino

acids 17-24). Samples were co-incubated in the plate overnight at 4°C along with a ruthenium-labeled anti-Aβ antibody specific for the C-terminal region of Aβ40 (ConFab40; Amgen). Plates were then washed, 150 µl/well read buffer T (MSD) was added and plates were read immediately on a Sector6000 imager according to manufacturer's recommended protocol (MSD). All samples were assayed in triplicate and analyzed using GraphPad Prism v. 5.04 (GraphPad Software Inc., LaJolla, CA). PD data was analyzed by one-way ANOVA and Dunnett's multiple comparison test. Dose-response data were fit using nonlinear regression analysis and EC_{50}s were calculated based on curve fitting.

In vivo pharmacokinetics studies

Femoral catheterized male Sprague-Dawley rats (250-275 g) were purchased from Taconic and were maintained on a 12 hour light/dark cycle with unrestricted access to food and water until use. Rats were fasted 7-12 hours prior to oral dose administration. The animals were dosed with compounds either orally as a solution or suspension in 2% HPMC and 1% Tween-80, pH 2 (10 mg/kg; 10 ml/kg dose volume) or intravenously (IV bolus) in DMSO at 2 mg/kg. Approximately 0.20 ml of whole blood was collected via the femoral vein catheter at 0.25, 0.5, 1, 2, 4, 6, 12, 16 and 24 hours post dose. Blood withdrawal volumes were within the IACUC Global Standards. Whole blood was centrifuged for plasma collection and stored at approximately -70°C until analysis.

In vivo pharmacodynamics studies

JPET Fast Forward. Published on August 21, 2012 as DOI: 10.1124/jpet.112.197954
This article has not been copyedited and formatted. The final version may differ from this version.

Male Sprague-Dawley rats (175-200 g) were dosed orally with compounds in 2% HPMC and 1% Tween-80, pH 2 at a volume of 10 ml/kg. For a typical compound screen, tissue samples were collected at a single 4 hour time point. Rats were euthanized with CO_2 inhalation for 2 minutes and the cisterna magna was quickly exposed by removing the skin and muscle above it. CSF (50-100 µl) was collected with a 30-gauge needle through the dura membrane covering the cisterna magna. CSF samples with visible blood contaminates were discarded. Blood was withdrawn by cardiac puncture and plasma obtained by centrifugation for drug concentration analysis. Brains were removed and, along with the CSF, immediately frozen on dry ice and stored at -80°C until use. The frozen brains were subsequently homogenized in 10 volumes (w/v) of freshly made 0.5% Triton X-100 in TBS in the presence of protease inhibitors. The homogenates were centrifuged at 355,000 x g for 30 min at 4°C. Pellets were discarded and supernatants stored at -80°C.

Measurement of plasma, CSF and brain drug concentration

Aliquots of plasma (50 µl) were combined with 300 µl of acetonitrile containing a structurally related internal standard (IS), vortexed and centrifuged 1,900 x g for 5 min. Supernatant (250 µl) was transferred into a 96 well plate for sample analysis. Aliquots of CSF (25 µl) were combined with 25 µl of acetonitrile. An additional 150 µl of acetonitrile containing a structurally related IS was added to each sample, vortexed and centrifuged 1,900 x g for 5 min. Supernatant (150 µl) was transferred into a 96 well plate for sample analysis.

JPET Fast Forward. Published on August 21, 2012 as DOI: 10.1124/jpet.112.197954
This article has not been copyedited and formatted. The final version may differ from this version.

Brain tissue samples were homogenized in 4 volumes of water (volume: tissue weight ratio) using a Covaris Acoustic Homogenizer. Aliquots of 50 µl of homogenate were combined with 300 µl of acetonitrile containing a structurally related IS, vortexed and centrifuged 1,900 x g for 5 min. Supernatant (250 µl) was transferred into a 96 well plate for sample analysis.

For plasma, CSF and brain homogenate, analytical standards were prepared in blank tissue or homogenate (for brain) and treated in an identical manner to the unknowns. Both standards and unknowns were measured by liquid chromatography mass spectrometry using Atmospheric Chemical Ionization (APCI) and multiple reaction monitoring in the positive ion mode.

Determination of plasma pharmacokinetic parameters

Individual plasma concentration-time data were analyzed by non-compartmental methods using Small Molecules Discovery Assay (SMDA) Watson® (version 7.0.0.01, InnaPhase Corp., Philadelphia, PA). Calculations were performed prior to rounding and nominal sampling times were used in the pharmacokinetic analysis. All pharmacokinetic parameters and summary statistics are reported to 3 significant figures, except for T_{max}. Oral bioavailability was calculated as F_{oral} (%) = 100 X [(PO $AUC_{0\text{-}inf}$/PO dose)/(IV $AUC_{0\text{-}inf}$/IV dose)].

JPET Fast Forward. Published on August 21, 2012 as DOI: 10.1124/jpet.112.197954
This article has not been copyedited and formatted. The final version may differ from this version.

Results

Using a combination of rational design and classical iterative optimization, we have established a clear structure-activity relationship (SAR) for BACE1 with a new series of potent, hydroxyethylamine (HEA)-based inhibitors (Dineen et al., 2012; Kaller et al., 2012; Weiss et al., 2012). Two lead compounds, N-((2S,3R)-1-(benzo[d][1,3]dioxol-5-yl)-3-hydroxy-4-(((S)-6'-neopentyl-3',4'-dihydrospiro[cyclobutane-1,2'-pyrano[2,3-b]pyridin]-4'-yl)amino)butan-2-yl)-2-methoxyacetamide (**Compound 1**) and (R)-N-((2S,3R)-3-hydroxy-4-(((S)-6'-neopentyl-3',4'-dihydrospiro[cyclobutane-1,2'-pyrano[2,3-b]pyridin]-4'-yl)amino)-1-(3-(thiazol-2-yl)phenyl)butan-2-yl)-2-methoxypropanamide (**Compound 2**) (Figure 1), were potent inhibitors in a FRET-based BACE1 enzyme assay, with IC_{50} values of 5.4 nM and 5.5 nM, respectively (Table 1). These compounds also showed significant inhibition of Aβ production in a cell-based assay using HEK293 cells stably transfected with APP containing the Swedish familial Alzheimer's disease (FAD) mutation (APPsw). In this assay, **Compound 1** had an IC_{50} of 16.8 nM and **Compound 2**, an IC_{50} of 9.6 nM resulting in cell:enzyme potency ratios of 3.1 and 1.8, respectively. In order to select appropriate candidates for *in vivo* pharmacodynamic (PD) studies in rats, all compounds were evaluated in a set of *in vitro* pharmacokinetic (PK) assays for passive permeability, rat P-gp mediated efflux and metabolic stability in rat liver microsomes (RLM). Both compounds showed high passive permeability with values of 25 x 10^{-6} cm/s and 17 x 10^{-6} cm/s for **Compound 1** and **Compound 2**, respectively. **Compound 1** showed high efflux via P-gp with an efflux ratio (ER) of 16.2 whereas **Compound 2** showed little or no P-gp mediated efflux with a ratio of 1.7. Additionally, **Compound 1** was less

JPET Fast Forward. Published on August 21, 2012 as DOI: 10.1124/jpet.112.197954
This article has not been copyedited and formatted. The final version may differ from this version.

metabolically stable than **Compound 2**. The intrinsic clearance measured in rat liver microsomes (RLM CL_{int}) was 140 µl/min/mg for **Compound 1** compared with 51 µl/min/mg for **Compound 2**. *In vivo*, both **Compound 1** and **Compound 2** displayed moderate clearance rates after intravenous (IV) dosing at 2 mg/kg in rats (1.25 L/h/kg and 0.87 L/h/kg, respectively). Oral dosing at 10 mg/kg in rats demonstrated that **Compound 1** and **Compound 2** are readily absorbed with plasma half-lives of 2.0 h and 1.0 h, respectively. The apparent bioavailability of both compounds was greater than 100%, a property that is attributed to non-linear pharmacokinetics (e.g. via saturable metabolism) at the 10 mg/kg oral dose relative to the lower 2 mg/kg IV dose (Table 1). Maximal plasma concentrations of 4.5 µM and 8.9 µM were achieved at 2 h and 5 h, respectively for **Compound 1** and **Compound 2** (data not shown). Combined with the fraction of drug unbound in plasma of 0.024 (**Compound 1**) and 0.014 (**Compound 2**), the unbound C_{max} was 0.108 µM and 0.125 µM for **Compound 1** and **Compound 2**, respectively. The unbound plasma C_{max} was 6-fold and 13-fold greater than the *in vitro* cell IC_{50}, and 20-fold and 23-fold greater than the enzyme IC_{50} (Table 1) for **Compound 1** and **Compound 2**, respectively.

To investigate the PD properties of BACE1 inhibitors *in vivo,* compounds were administered in a single oral dose to Sprague-Dawley rats and Aβ40 levels measured in CSF and brain tissue. Substantial Aβ40 lowering in both compartments was observed in a dose-dependent manner for both compounds 4 hours post drug administration (Figure 2). For **Compound 1**, the total plasma EC_{50} values for CSF (CSF EC_{50}) and brain (brain EC_{50}) Aβ40 lowering were 5.8 µM and 17.0 µM, respectively. For **Compound 2**, CSF EC_{50} and brain EC_{50} values were 1.6 µM and 4.5 µM, respectively. Factoring in

JPET Fast Forward. Published on August 21, 2012 as DOI: 10.1124/jpet.112.197954
This article has not been copyedited and formatted. The final version may differ from this version.

protein binding in plasma, the estimated unbound plasma EC_{50} for CSF Aβ40 lowering was 0.140 μM or approximately 8-fold higher than the BACE cell IC_{50} for **Compound 1** and 0.023 μM or approximately 2-fold higher than the BACE cell IC_{50} for **Compound 2**. The EC_{50}s calculated for both CSF and brain Aβ40 lowering were greater for **Compound 1** than those observed for **Compound 2**, consistent with the higher efflux ratio of **Compound 1**. A time course experiment was also conducted with **Compound 2** to further evaluate the PK-PD relationship for this compound (Figure 3). Rats were dosed at 30 mg/kg and samples collected at the indicated time points and analyzed for both drug and Aβ40 levels. A 30 mg/kg dose was chosen because it was predicted to produce a transient, robust inhibition of CSF Aβ levels based on prior PK and PD data (not shown). There was a clear relationship between unbound plasma drug concentrations, CSF drug concentrations and Aβ lowering in the brain and CSF. Significant Aβ40 reduction was observed in CSF at 2 h and in brain 1 h after dosing ($p < 0.01$). The maximum reduction in Aβ40 levels were observed at 4 h in both CSF (86%) and brain (73%). Aβ40 levels in both CSF and brain returned to baseline 12 h after dosing. Note that the measurement of drug in CSF at the 12 h time point fell below the limit of detection (0.002 μM). The dynamic ranges of measurement for drug and Aβ40 in CSF, plasma and brain homogenate, including limits of detection, are shown in Supplemental Table 2.

Assessment of > 100 compounds that were analyzed *in vivo* provided insights into how various *in vitro* characteristics translated into PD effects *in vivo*. *In vivo* PD dose response curves were generated for 48 compounds. A comparison of the CSF EC_{50} for Aβ40 reduction with the brain EC_{50} for these compounds (Figure 4) displayed a

linear relationship with good correlation between the Aβ40 reduction in the 2 compartments (r^2 = 0.778; $p < 0.0001$; n = 48). A plot of *in vitro* cell potency versus *in vivo* PD effect indicated no relationship between Aβ inhibition *in vitro* and *in vivo* (r^2 = 0.008; not significant; Figure 5A). This is likely due to the wide ranges of metabolic stability, permeability and efflux ratios associated with these compounds. However, when *in vivo* exposure was factored in, a clear relationship was observed. As the ratio of plasma drug levels relative to *in vitro* potency increased, the degree of CSF Aβ lowering increased (4 h time point following a single 30 mg/kg oral dose of each compound) (r^2 = 0.26; $p < 0.0001$) (Figure 5B)**.**

In order to more clearly illustrate the impact of several key *in vitro* PK parameters on *in vivo* potency, compound PD effects were binned into 3 categories: inactive (CSF Aβ reduction $\leq$ 25%), moderately active (CSF Aβ reduction of 25-50%) and highly active (CSF Aβ reduction > 50%). The percentage of compounds in each activity bin was examined as function of *in vitro* PK parameters (Figure 6). To mitigate the influence of pharmacological potency, this evaluation included only compounds with potencies of < 30 nM in the cell-based assay (n = 104). Figure 6A shows a clear relationship between permeability and CSF Aβ reduction, with the most permeable compounds producing the largest reduction in CSF Aβ levels. In the set of compounds with permeability values > 20 x 10^{-6} cm/sec, 48% were highly active, and 26% were inactive. In contrast, 75% of compounds with passive permeability values < 10 x 10^{-6} cm/sec were inactive and none were highly active. The effect of rat P-gp efflux on *in vivo* potency was also pronounced (Figure 6B). As the efflux ratio (ER) increased, the percentage of active compounds decreased and the percentage of inactive compounds increased. Nearly all compounds

(97.6%) that showed no significant P-gp mediated efflux (ER < 3) demonstrated central nervous system (CNS) activity (≥ 25% Aβ reduction); 74% inhibited CSF Aβ by more than 50%. The majority of compounds (86.7%) that showed moderate P-gp mediated efflux (ER = 3-10) were active in the CNS; 67% were highly active. The percentage of highly active compounds dropped significantly once efflux ratios exceeded 10. Only 9% of compounds with efflux ratios between 10 and 30, and no compounds with efflux ratios > 30 were highly active. This efflux effect was also apparent in the moderately active compound group. A similar trend was observed for compound stability measured in rat liver microsomes (Figure 6C). As RLM CL_{int} values increased, the percentage of active compounds decreased and the percentage of inactive compounds increased. Sixty-five percent of compounds with RLM CL_{int} values < 100 μl/min/mg were highly active as opposed to only 14% of compounds with RLM CL_{int} values > 100 μl/min/mg.

Within the 3 activity bins, average values for permeability, efflux ratio and RLM CL_{int} were calculated and compared (Supplemental Table 1). As expected, an inverse relationship was observed between efflux ratio and CSF Aβ reduction. Mean efflux ratios ranged from 32.2 in the inactive bin to 10.3 in the moderately active bin to 2.8 in the highly active bin with mean differences between the inactive and highly active bins reaching statistical significance (adjusted p-value = 0.0004). Likewise, an inverse relationship was also observed for RLM CL_{int} values and CSF Aβ reduction. Mean RLM CL_{int} values ranged from 194.7 μl/min/mg in the inactive bin to 172.6 μl/min/mg in the moderately active bin to 92.9 μl/min/mg in the highly active bin. Mean differences between the inactive and highly active bins (adjusted p-value < 0.0001) and between the moderately active and highly active bins (adjusted p-value = 0.0002) reached

statistical significance. With this set of compounds, the range of permeability values covered in these studies was relatively narrow, (mean permeability of the inactive group was 19.0 10^{-6} cm/s compared with 22.5 10^{-6} cm/s for the highly active group), however, overall the data suggests that high permeability is necessary but not sufficient to drive Aβ reduction in the brain.

Discussion

One of the biggest challenges encountered with small molecule BACE1 inhibitors is obtaining good passive permeability across the blood-brain barrier (BBB) while avoiding P-gp-mediated efflux. BACE inhibitors that are subject to P-gp efflux would be predicted to deliver unbound drug levels in the brain significantly lower than unbound drug levels in the plasma based on basic physiological principles governing permeation of small molecules across the blood-brain barrier and supported by published data on marketed drugs (Mahar Doan et al., 2002). Indeed, recent reports show that BACE1 inhibitors that are also good P-gp substrates can effectively lower brain Aβ only in the presence of a P-gp inhibitor or in P-gp knock-out mice (Hussain et al., 2007; Sankaranarayanan et al., 2009; Thompson et al., 2011). Much is now understood regarding the relationship of various physicochemical properties of small molecules (eg. cLogP, polar surface area, number of hydrogen-bond donors, etc.) to P-gp efflux which has enabled medicinal chemists to engineer molecules with desirable efflux properties (Hitchcock, 2012). In addition to compound properties that permit good blood-brain barrier permeation, an ideal BACE1 inhibitor therapeutic would also be orally bioavailable and have sufficiently low hepatic clearance to enable it to achieve and maintain adequate plasma concentrations. Indeed aspartyl protease inhibitors in general (e.g. HIV, BACE1 and renin) have tended to suffer from high *in vivo* clearance and poor *in vitro* metabolic stability in hepatic microsomal assays amended with the appropriate co-factors to support oxidative metabolism. This phenomenon can likely be attributed to the peptidomimetic nature of these aspartyl protease inhibitors. In this

report, we have carefully explored the PK-PD relationship across a large series of novel, orally bioavailable, brain-penetrant BACE1 inhibitors.

Compound 1 and **2** are both potent inhibitors of BACE1 in enzyme and cell-based assays. Both compounds have high *in vitro* permeability and moderate *in vivo* clearance in rat. **Compound 1** and **2** both have oral bioavailability > 100% due to non-linear pharmacokinetics and saturable metabolism. However, **Compound 2** has a low efflux ratio, while **Compound 1** has high efflux, allowing us to assess the effect of efflux on Aβ40 inhibition in the CSF and brain. As expected, the total plasma EC_{50} values for CSF and brain Aβ40 inhibition for **Compound 1** were 3.6- and 3.8-fold higher than the corresponding values for **Compound 2**. Furthermore, after correction for plasma protein binding, the ratio between the *in vivo* unbound plasma EC_{50} for CSF Aβ40 inhibition and the *in vitro* cell IC_{50} was much higher for **Compound 1** than for **Compound 2** (8-fold vs 2-fold), consistent with a significant reduction in central efficacy caused by P-gp mediated efflux.

Although both compounds showed dose-dependent reduction of Aβ levels in brain homogenate and CSF after oral dosing, in both cases the apparent EC_{50} for brain effect was larger than the EC_{50} determined from CSF data, suggesting differential potency in the two CNS compartments. This apparent brain/CSF shift has been observed by others with both BACE1 and gamma secretase inhibitors (Dineen et al., 2012; Hawkins et al., 2011; Lu et al., 2011; Sankaranarayanan et al., 2009; Weiss et al., 2012). There are several possible explanations for this observation. The first is that each compartment has active BACE1 and generates Aβ at least partially independently from one another (Crossgrove et al., 2007). In this model it would be possible for

different inhibitor potencies *in vivo* due to different exposure of drug in the 2 compartments. However, evidence suggests that Aβ is produced primarily in brain tissue. Following secretion from neurons, Aβ that is not enzymatically degraded is thought to drain through the extracellular space into CSF, presumably with some time lag. In studies using a single administration of compound, the amount of Aβ inhibition varies with drug concentration, as shown in Figure 3. The amount of Aβ reduction observed in CSF may reflect the amount of Aβ reduction in brain at an earlier point in time. If Aβ is assessed at a point in time during which drug levels in the brain compartment are decreasing, the apparent inhibition in CSF will exceed that observed in brain tissue. If Aβ is measured at a time during which drug levels are increasing in brain, the reverse would be true. Recent PK-PD modeling of Aβ reduction in brain and CSF following secretase inhibition supports this disparity in Aβ turnover kinetics between the two compartments (Lu et al., 2012).

Drug development programs often focus on trying to improve compound potency. Early HEA-based inhibitors showed good inhibitory potency in biochemical and cell-based assays, however they were not effective *in vivo* (Freskos et al., 2007; Kortum et al., 2007; Maillard et al., 2007; Stachel et al., 2004). Our data shows that although potency is clearly important, within a series of 134 compounds with potency < 100 nM (and most < 30 nM), there was no correlation between *in vivo* PD efficacy and *in vitro* potency. Further analysis of PK-PD data from 104 potent compounds (all < 30 nM cell IC_{50}) showed the importance of efflux, permeability and microsomal clearance for the efficacy of BACE1 inhibitors in the brain. Not surprisingly for this target, there was a very strong inverse relationship between P-gp mediated efflux and CSF and brain Aβ40

inhibition. No compounds with efflux ratios over 30, and only 9% of compounds with efflux ratios between 10 and 30 showed over 50% inhibition of CSF Aβ40 levels. In contrast, 74% of compounds with efflux ratios less than 3 produced greater than 50% Aβ40 inhibition in CSF. Similarly, no compounds with permeability less than 10 x 10^{-6} cm/s produced efficacy greater than 50% Aβ40 inhibition in CSF, and only 25% demonstrated efficacy in the 25-50% inhibition range. Finally, the importance of metabolic stability was also evident in this set of BACE1 inhibitors as the fraction of highly active compounds with RLM CL_{int} values < 100 µl/min/mg (65%) was significantly greater than the percentage of highly active compounds with RLM CL_{int} values > 100 µl/min/mg (14%). The optimal BACE1 inhibitor based on this data set would have a cell IC_{50} value less than 30 nM, P-gp efflux ratio less than 3, permeability greater than 20 x 10^{-6} cm/s and RLM CL_{int} less than 50 µl/min/mg. Seven compounds met all 4 criteria and they inhibited CSF Aβ40 levels by 61-80% 4 hours after a single 30 mg/kg oral dose, with a mean reduction of 70%. The EC_{50}s for CSF Aβ40 inhibition for the same 7 compounds ranged from 1.3 µM to 6.5 µM. A translation of this approach to guiding Aβ reduction in the clinic should be possible as human versions of all 3 *in vitro* PK assays described here are available.

Acknowledgments

The authors would like to thank Jessie Gu for the statistical analysis.

Authorship Contributions

Participated in research design: *Wood, Wen, Hitchcock, Citron, Hickman, Zhong and Williamson*
Conducted experiments: *Zhang, Zhu, Babu-Khan, Chen, Pham, Esmay and Luo*
Contributed new reagents or analytic tools: *Dineen, Kaller, Weiss and Zhong*
Performed data analysis: *Wood, Wen, Babu-Khan, Chen, Pham, Esmay, Luo, Hitchcock, Hickman and Williamson*
Wrote or contributed to the writing of the manuscript: *Wood, Wen, Chen, Pham, Esmay, Dineen, Kaller, Weiss, Hitchcock, Citron, Zhong, Hickman and Williamson*

References

Best JD, Jay MT, Otu F, Ma J, Nadin A, Ellis S, Lewis HD, Pattison C, Reilly M, Harrison T, Shearman MS, Williamson TL and Atack JR (2005) Quantitative measurement of changes in amyloid-beta(40) in the rat brain and cerebrospinal fluid following treatment with the gamma-secretase inhibitor LY-411575 [N2-[(2S)-2-(3,5-difluorophenyl)-2-hydroxyethanoyl]-N1-[(7S)-5-methyl-6-oxo-6,7-d ihydro-5H-dibenzo[b,d]azepin-7-yl]-L-alaninamide]. *J Pharmacol Exp Ther* **313**:902-908.

Booth-Genthe CL, Louie SW, Carlini EJ, Li B, Leake BF, Eisenhandler R, Hochman JH, Mei Q, Kim RB, Rushmore TH and Yamazaki M (2006) Development and characterization of LLC-PK1 cells containing Sprague-Dawley rat Abcb1a (Mdr1a): comparison of rat P-glycoprotein transport to human and mouse. *J Pharmacol Toxicol Methods* **54**:78-89.

Chakrabarti E, Ghosh S, Sadhukhan S, Sayre L, Tochtrop GP and Smith JD (2010) Synthesis and biological evaluation of analogues of a novel inhibitor of beta-amyloid secretion. *J Med Chem* **53**:5302-5319.

Charrier N, Clarke B, Cutler L, Demont E, Dingwall C, Dunsdon R, Hawkins J, Howes C, Hubbard J, Hussain I, Maile G, Matico R, Mosley J, Naylor A, O'Brien A, Redshaw S, Rowland P, Soleil V, Smith KJ, Sweitzer S, Theobald P, Vesey D, Walter DS and Wayne G (2009) Second generation of BACE-1 inhibitors. Part 1: The need for improved pharmacokinetics. *Bioorg Med Chem Lett* **19**:3664-3668.

Citron M (2010) Alzheimer's disease: strategies for disease modification. *Nat Rev Drug Discov* **9**:387-398.

Crossgrove JS, Smith EL and Zheng W (2007) Macromolecules involved in production and metabolism of beta-amyloid at the brain barriers. *Brain Res* **1138**:187-195.

Dineen TA, Weiss MM, Williamson T, Acton P, Babu-Khan S, Bartberger MD, Brown J, Chen K, Cheng Y, Citron M, Croghan MD, Dunn RT, 2nd, Esmay J, Graceffa RF, Harried SS, Hickman D, Hitchcock SA, Horne DB, Huang H, Imbeah-Ampiah R, Judd T, Kaller MR, Kreiman CR, La DS, Li V, Lopez P, Louie S, Monenschein H, Nguyen TT, Pennington LD, San Miguel T, Sickmier EA, Vargas HM, Wahl RC, Wen PH, Whittington DA, Wood S, Xue Q, Yang BH, Patel VF and Zhong W (2012) Design and Synthesis of Potent, Orally Efficacious Hydroxyethylamine Derived beta-Site Amyloid Precursor Protein Cleaving Enzyme (BACE1) Inhibitors. *J Med Chem*.

Freskos JN, Fobian YM, Benson TE, Bienkowski MJ, Brown DL, Emmons TL, Heintz R, Laborde A, McDonald JJ, Mischke BV, Molyneaux JM, Moon JB, Mullins PB, Bryan Prince D, Paddock DJ, Tomasselli AG and Winterrowd G (2007) Design of potent inhibitors of human beta-secretase. Part 1. *Bioorg Med Chem Lett* **17**:73-77.

Fukumoto H, Takahashi H, Tarui N, Matsui J, Tomita T, Hirode M, Sagayama M, Maeda R, Kawamoto M, Hirai K, Terauchi J, Sakura Y, Kakihana M, Kato K, Iwatsubo T and Miyamoto M (2010) A noncompetitive BACE1 inhibitor TAK-070 ameliorates Abeta pathology and behavioral deficits in a mouse model of Alzheimer's disease. *J Neurosci* **30**:11157-11166.

Ghosh AK, Brindisi M and Tang J (2012) Developing beta-secretase inhibitors for treatment of Alzheimer's disease. *J Neurochem* **120 Suppl 1**:71-83.

Hardy J and Selkoe DJ (2002) The amyloid hypothesis of Alzheimer's disease: progress and problems on the road to therapeutics. *Science* **297**:353-356.

Hawkins J, Harrison DC, Ahmed S, Davis RP, Chapman T, Marshall I, Smith B, Mead TL, Medhurst A, Giblin GM, Hall A, Gonzalez MI, Richardson J and Hussain I (2011) Dynamics of Abeta42 reduction in plasma, CSF and brain of rats treated with the gamma-secretase modulator, GSM-10h. *Neurodegener Dis* **8**:455-464.

Hitchcock SA (2012) Structural Modifications that Alter the P-Glycoprotein Efflux Properties of Compounds. *J Med Chem* **55**:4877-4895.

Hong L, Koelsch G, Lin X, Wu S, Terzyan S, Ghosh AK, Zhang XC and Tang J (2000) Structure of the protease domain of memapsin 2 (beta-secretase) complexed with inhibitor. *Science* **290**:150-153.

Hussain I, Hawkins J, Harrison D, Hille C, Wayne G, Cutler L, Buck T, Walter D, Demont E, Howes C, Naylor A, Jeffrey P, Gonzalez MI, Dingwall C, Michel A, Redshaw S and Davis JB (2007) Oral administration of a potent and selective non-peptidic BACE-1 inhibitor decreases beta-cleavage of amyloid precursor protein and amyloid-beta production in vivo. *J Neurochem* **100**:802-809.

Kaller MR, Harried SS, Albrecht B, Amarante P, Babu-Khan S, Bartberger MD, Brown J, Brown R, Chen K, Cheng Y, Citron M, Croghan MD, Graceffa RF, Hickman D, Judd T, Kriemen C, La DS, Li V, Lopez P, Luo Y, Masse C, Monenschein H, Nguyen TT, Pennington LD, San Miguel T, Sickmier EA, Wahl RC, Weiss MM, Wen PH, Williamson T, Wood S, Xue M, Yang BH, Zhang J, Patel VF, Zhong W and Hitchcock S (2012) A Potent and Orally Efficacious, Hydroxyethylamine-Based Inhibitor of β-Secretase. *ACS Med Chem Lett*.

Kortum SW, Benson TE, Bienkowski MJ, Emmons TL, Prince DB, Paddock DJ, Tomasselli AG, Moon JB, LaBorde A and TenBrink RE (2007) Potent and selective isophthalamide S2 hydroxyethylamine inhibitors of BACE1. *Bioorg Med Chem Lett* **17**:3378-3383.

Lu Y, Riddell D, Hajos-Korcsok E, Bales K, Wood KM, Nolan CE, Robshaw AE, Zhang L, Leung L, Becker SL, Tseng E, Barricklow J, Miller EH, Osgood S, O'Neill BT, Brodney MA, Johnson DS and Pettersson M (2012) Cerebrospinal Fluid Amyloid-beta (Abeta) as an Effect Biomarker for Brain Abeta Lowering Verified by Quantitative Preclinical Analyses. *J Pharmacol Exp Ther* **342**:366-375.

Lu Y, Zhang L, Nolan CE, Becker SL, Atchison K, Robshaw AE, Pustilnik LR, Osgood SM, Miller EH, Stepan AF, Subramanyam C, Efremov I, Hallgren AJ and Riddell D (2011) Quantitative pharmacokinetic/pharmacodynamic analyses suggest that the 129/SVE mouse is a suitable preclinical pharmacology model for identifying small-molecule gamma-secretase inhibitors. *J Pharmacol Exp Ther* **339**:922-934.

Mahar Doan KM, Humphreys JE, Webster LO, Wring SA, Shampine LJ, Serabjit-Singh CJ, Adkison KK and Polli JW (2002) Passive permeability and P-glycoprotein-mediated efflux differentiate central nervous system (CNS) and non-CNS marketed drugs. *J Pharmacol Exp Ther* **303**:1029-1037.

Maillard MC, Hom RK, Benson TE, Moon JB, Mamo S, Bienkowski M, Tomasselli AG, Woods DD, Prince DB, Paddock DJ, Emmons TL, Tucker JA, Dappen MS, Brogley L, Thorsett ED, Jewett N, Sinha S and John V (2007) Design, synthesis, and crystal structure of hydroxyethyl secondary amine-based peptidomimetic inhibitors of human beta-secretase. *J Med Chem* **50**:776-781.

Malamas MS, Erdei J, Gunawan I, Turner J, Hu Y, Wagner E, Fan K, Chopra R, Olland A, Bard J, Jacobsen S, Magolda RL, Pangalos M and Robichaud AJ (2010) Design and synthesis

of 5,5'-disubstituted aminohydantoins as potent and selective human beta-secretase (BACE1) inhibitors. *J Med Chem* **53**:1146-1158.

May PC, Dean RA, Lowe SL, Martenyi F, Sheehan SM, Boggs LN, Monk SA, Mathes BM, Mergott DJ, Watson BM, Stout SL, Timm DE, Smith Labell E, Gonzales CR, Nakano M, Jhee SS, Yen M, Ereshefsky L, Lindstrom TD, Calligaro DO, Cocke PJ, Greg Hall D, Friedrich S, Citron M and Audia JE (2011) Robust Central Reduction of Amyloid-beta in Humans with an Orally Available, Non-Peptidic beta-Secretase Inhibitor. *J Neurosci* **31**:16507-16516.

Sankaranarayanan S, Holahan MA, Colussi D, Crouthamel MC, Devanarayan V, Ellis J, Espeseth A, Gates AT, Graham SL, Gregro AR, Hazuda D, Hochman JH, Holloway K, Jin L, Kahana J, Lai MT, Lineberger J, McGaughey G, Moore KP, Nantermet P, Pietrak B, Price EA, Rajapakse H, Stauffer S, Steinbeiser MA, Seabrook G, Selnick HG, Shi XP, Stanton MG, Swestock J, Tugusheva K, Tyler KX, Vacca JP, Wong J, Wu G, Xu M, Cook JJ and Simon AJ (2009) First demonstration of cerebrospinal fluid and plasma A beta lowering with oral administration of a beta-site amyloid precursor protein-cleaving enzyme 1 inhibitor in nonhuman primates. *J Pharmacol Exp Ther* **328**:131-140.

Stachel SJ, Coburn CA, Rush D, Jones KL, Zhu H, Rajapakse H, Graham SL, Simon A, Katharine Holloway M, Allison TJ, Munshi SK, Espeseth AS, Zuck P, Colussi D, Wolfe A, Pietrak BL, Lai MT and Vacca JP (2009) Discovery of aminoheterocycles as a novel beta-secretase inhibitor class: pH dependence on binding activity part 1. *Bioorg Med Chem Lett* **19**:2977-2980.

Stachel SJ, Coburn CA, Steele TG, Jones KG, Loutzenhiser EF, Gregro AR, Rajapakse HA, Lai MT, Crouthamel MC, Xu M, Tugusheva K, Lineberger JE, Pietrak BL, Espeseth AS, Shi XP, Chen-Dodson E, Holloway MK, Munshi S, Simon AJ, Kuo L and Vacca JP (2004) Structure-based design of potent and selective cell-permeable inhibitors of human beta-secretase (BACE-1). *J Med Chem* **47**:6447-6450.

Thompson LA, Shi J, Decicco CP, Tebben AJ, Olson RE, Boy KM, Guernon JM, Good AC, Liauw A, Zheng C, Copeland RA, Combs AP, Trainor GL, Camac DM, Muckelbauer JK, Lentz KA, Grace JE, Burton CR, Toyn JH, Barten DM, Marcinkeviciene J, Meredith JE, Albright CF and Macor JE (2011) Synthesis and in vivo evaluation of cyclic diaminopropane BACE-1 inhibitors. *Bioorg Med Chem Lett* **21**:6909-6915.

Truong AP, Toth G, Probst GD, Sealy JM, Bowers S, Wone DW, Dressen D, Hom RK, Konradi AW, Sham HL, Wu J, Peterson BT, Ruslim L, Bova MP, Kholodenko D, Motter RN, Bard F, Santiago P, Ni H, Chian D, Soriano F, Cole T, Brigham EF, Wong K, Zmolek W, Goldbach E, Samant B, Chen L, Zhang H, Nakamura DF, Quinn KP, Yednock TA and Sauer JM (2010) Design of an orally efficacious hydroxyethylamine (HEA) BACE-1 inhibitor in a preclinical animal model. *Bioorg Med Chem Lett* **20**:6231-6236.

Turner RT, 3rd, Koelsch G, Hong L, Castanheira P, Ermolieff J, Ghosh AK and Tang J (2001) Subsite specificity of memapsin 2 (beta-secretase): implications for inhibitor design. *Biochemistry* **40**:10001-10006.

Vassar R, Bennett BD, Babu-Khan S, Kahn S, Mendiaz EA, Denis P, Teplow DB, Ross S, Amarante P, Loeloff R, Luo Y, Fisher S, Fuller J, Edenson S, Lile J, Jarosinski MA, Biere AL, Curran E, Burgess T, Louis JC, Collins F, Treanor J, Rogers G and Citron M (1999) Beta-secretase cleavage of Alzheimer's amyloid precursor protein by the transmembrane aspartic protease BACE. *Science* **286**:735-741.

Vassar R and Kandalepas PC (2011) The beta-secretase enzyme BACE1 as a therapeutic target for Alzheimer's disease. *Alzheimers Res Ther* **3**:20.

Weiss MM, Williamson T, Babu-Khan S, Bartberger MD, Brown J, Chen K, Cheng Y, Citron M, Croghan MD, Dineen TA, Esmay J, Graceffa RF, Harried SS, Hickman D, Hitchcock SA, Horne DB, Huang H, Imbeah-Ampiah R, Judd T, Kaller MR, Kreiman CR, La DS, Li V, Lopez P, Louie S, Monenschein H, Nguyen TT, Pennington LD, Rattan C, San Miguel T, Sickmier EA, Wahl RC, Wen PH, Wood S, Xue Q, Yang BH, Patel VF and Zhong W (2012) Design and Preparation of a Potent Series of Hydroxyethylamine Containing beta-Secretase Inhibitors That Demonstrate Robust Reduction of Central beta-Amyloid. *J Med Chem*.

Yang HC, Chai X, Mosior M, Kohn W, Boggs LN, Erickson JA, McClure DB, Yeh WK, Zhang L, Gonzalez-DeWhitt P, Mayer JP, Martin JA, Hu J, Chen SH, Bueno AB, Little SP, McCarthy JR and May PC (2004) Biochemical and kinetic characterization of BACE1: investigation into the putative species-specificity for beta- and beta'-cleavage sites by human and murine BACE1. *J Neurochem* **91**:1249-1259.

Footnotes

[1]Currently at Amgen, Dept. of Global Regulatory Affairs & Safety

[2]Currently at Envoy Therapeutics, 555 Heritage Drive, Jupiter Florida 33458

[3]Currently at UCB Pharma, Brussels, Belgium

[4]Currently at Amgen, Dept. of Comparative Biology & Safety Sciences

Figure Legends

Figure 1 Structures of **Compound 1** and **Compound 2**, hydroxylethylamine (HEA)-derived BACE1 inhibitors.

Figure 2 **Compounds 1** and **2** demonstrated concentration dependent lowering of CSF (filled circles) and brain (open triangles) Aβ40 levels relative to vehicle controls when dosed orally to wild type Sprague-Dawley rats. Each symbol represents a measurement from an individual rat (n = 5/dose group). Compounds were dosed at various concentrations in 2% HPMC and 1% Tween-80 at pH 2. Aβ and compound concentrations were measured 4 h post-dose.

Figure 3 Time course experiment demonstrating pharmacokinetic-pharmacodynamic (PK-PD) relationship for **Compound 2**. Rats were dosed at 30 mg/kg and samples were analyzed for both drug and Aβ40 levels at indicated time points. **A)** PK-PD relationship between Aβ40 (filled circles, black line) and drug levels in CSF (open squares, grey line). Note that the measurement of drug in CSF at the 12h time point fell below our limit of detection (0.002 μM; see Supplemental Table 2) **B)** PK-PD relationship between Aβ40 (filled circles, black line) levels in brain and unbound plasma drug levels (open squares, grey line). Data plotted are averages with standard deviations (n = 5).

JPET Fast Forward. Published on August 21, 2012 as DOI: 10.1124/jpet.112.197954
This article has not been copyedited and formatted. The final version may differ from this version.

Figure 4 *In vivo* dose response curves were generated for 48 compounds and EC_{50}s for brain and CSF Aβ lowering were calculated. A comparison of CSF EC_{50} and brain EC_{50} for these compounds shows a positive, linear relationship between the 2 compartments ($r^2 = 0.778$; $p < 0.0001$; $n = 48$).

Figure 5 **A)** Comparison of *in vitro* potency (cell IC_{50}) with *in vivo* PD effect indicated no clear relationship between Aβ inhibition *in vitro* and *in vivo* ($r^2 = 0.008$; $p = 0.3111$)**.** **B)** Comparison of plasma drug concentration (total) relative to *in vitro* potency and *in vivo* PD effect showed a clear relationship ($r^2 = 0.26$; $p < 0.0001$)**.** All compounds ($n = 134$) were dosed orally at 30 mg/kg and CSF Aβ40 and plasma drug levels were measured 4 h post-dose.

Figure 6 Compound PD effects were binned into 3 categories: inactive (CSF Aβ reduction $\leq$ 25%; black bars), moderately active (CSF Aβ reduction of 25-50%; dark grey bars) and highly active (CSF Aβ reduction > 50%; light grey bars). The percentage of compounds in each activity bin was calculated as function of **A)** passive permeability (Permeability), **B)** P-gp mediated efflux (Efflux Ratio) and **C)** metabolic stability in rat liver microsomes (RLM CL_{int}).

JPET Fast Forward. Published on August 21, 2012 as DOI: 10.1124/jpet.112.197954
This article has not been copyedited and formatted. The final version may differ from this version.

Table 1

Pharmacokinetic and pharmacodynamic properties of **Compound 1** and **Compound 2**.

	Compound 1	**Compound 2**
BACE1 FRET IC_{50} (nM)	5.4	5.5
BACE1 Cell IC_{50} (nM)	16.8	9.6
Permeability (10^6 cm/s)	25	17
Rat P-gp Efflux Ratio	16.2	1.7
RLM CL_{int} (μl/min/mg)	140	51
Rat (IV) Clearance (L/h/kg)	1.25	0.87
%F	> 100	> 100
Rat (Oral) $T_{1/2}$ (h)	2.0	1.0

Figure 1.

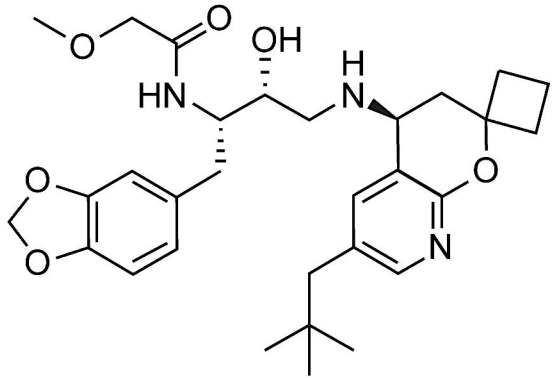

Compound 1

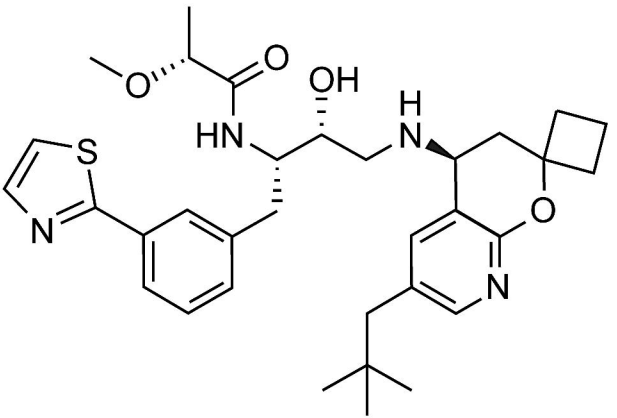

Compound 2

Figure 2.

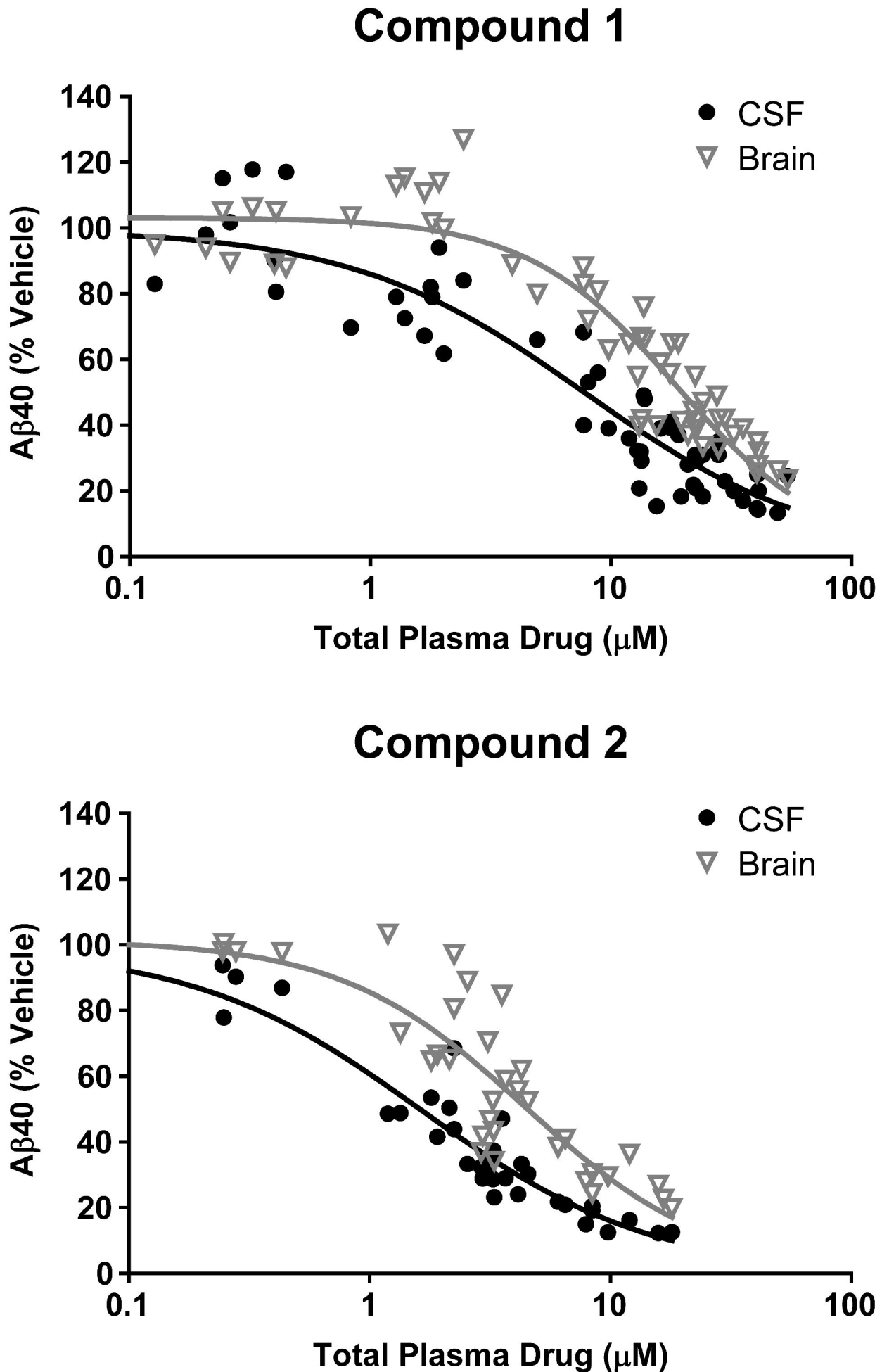
Compound 1
CSF
Brain
Aβ40 (% Vehicle)
140
120
100
80
60
40
20
0
0.1
1
10
100
Total Plasma Drug (μM)
Compound 2
CSF
Brain
Aβ40 (% Vehicle)
140
120
100
80
60
40
20
0
0.1
1
10
100
Total Plasma Drug (μM)

Figure 3.

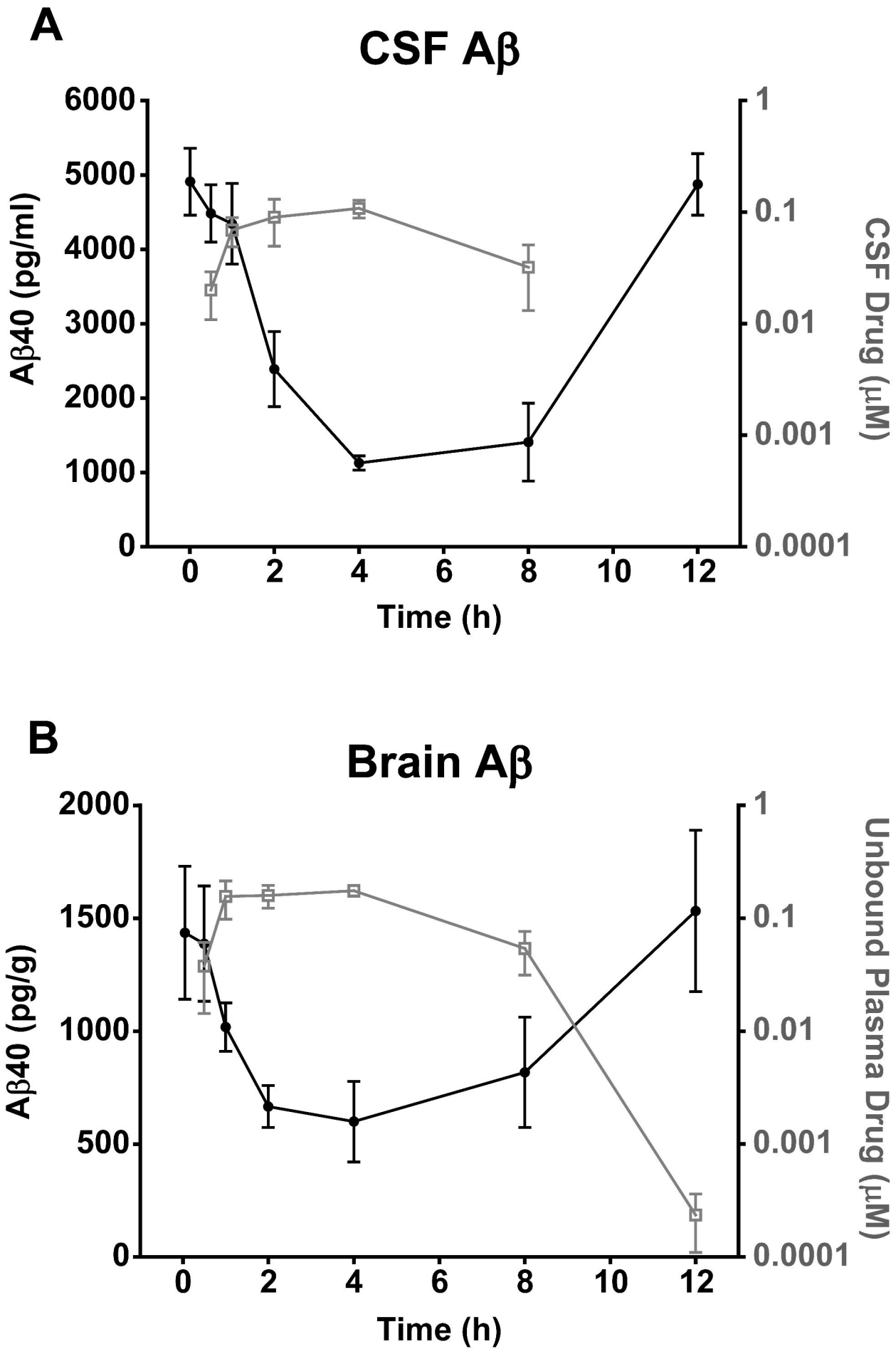
A
CSF Aβ
Aβ40 (pg/ml)
CSF Drug (μM)
Time (h)
B
Brain Aβ
Aβ40 (pg/g)
Unbound Plasma Drug (μM)
Time (h)

Figure 4.

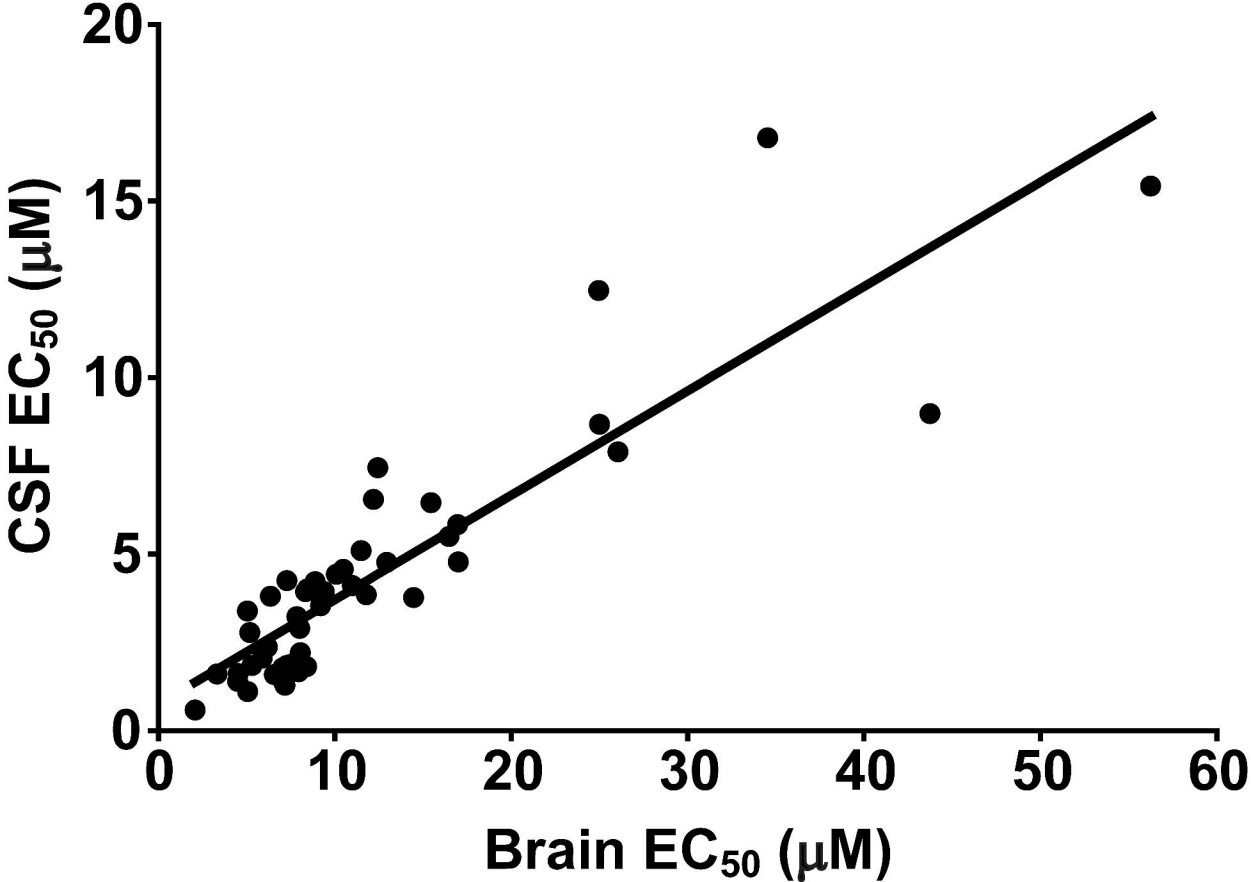

Figure 5.

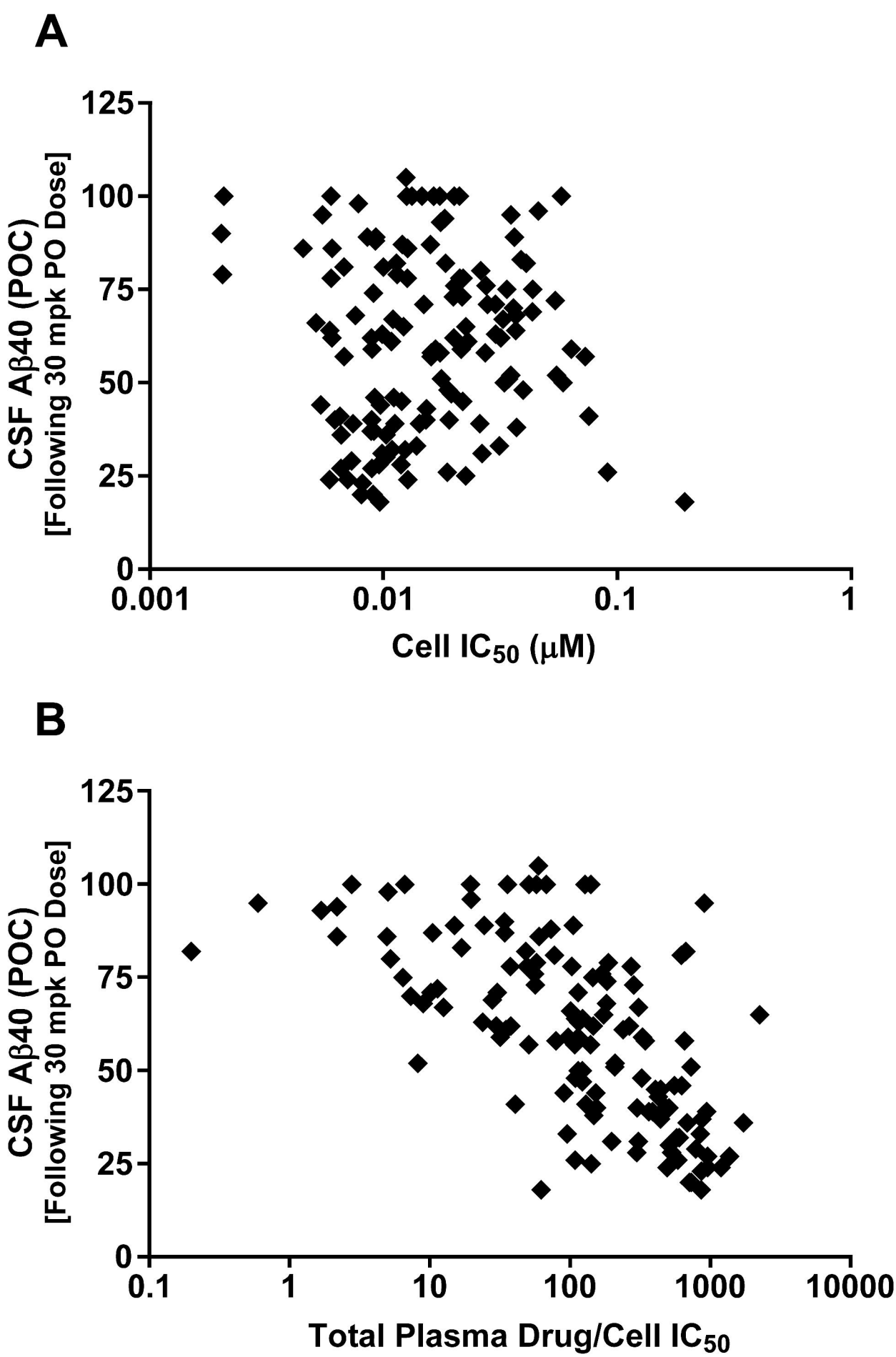
A
125
100
75
50
25
0
CSF Aβ40 (POC)
[Following 30 mpk PO Dose]
0.001
0.01
0.1
1
Cell IC50 (μM)
B
125
100
75
50
25
0
CSF Aβ40 (POC)
[Following 30 mpk PO Dose]
0.1
1
10
100
1000
10000
Total Plasma Drug/Cell IC50

Figure 6.

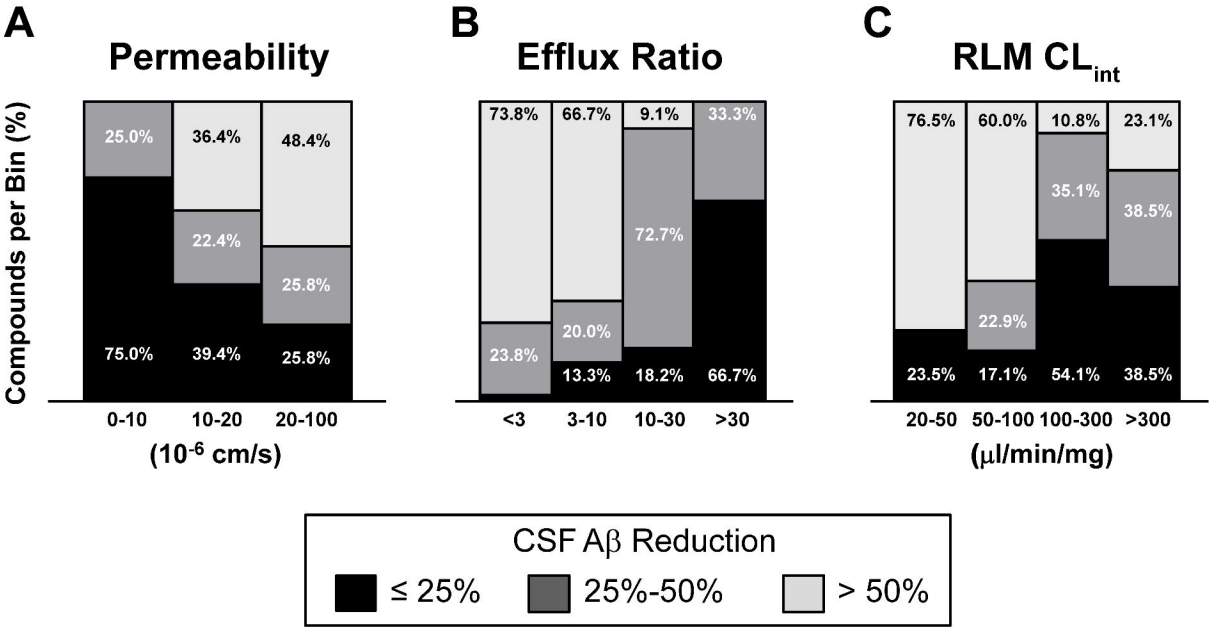
A
Permeability
Compounds per Bin (%)
25.0%
36.4%
48.4%
22.4%
25.8%
75.0%
39.4%
25.8%
0-10
10-20
20-100
(10-6 cm/s)
B
Efflux Ratio
73.8%
66.7%
9.1%
33.3%
72.7%
20.0%
23.8%
13.3%
18.2%
66.7%
<3
3-10
10-30
>30
C
RLM CLint
76.5%
60.0%
10.8%
23.1%
35.1%
38.5%
22.9%
23.5%
17.1%
54.1%
38.5%
20-50
50-100
100-300
>300
(µl/min/mg)
CSF Aβ Reduction
≤ 25%
25%-50%
> 50%